Structure and magnetic properties of $La_{1-x}Ce_xFe_{10.4}Si_{2.6}$ compounds

1997 J. Phys.: Condens. Matter 9 7463

(http://iopscience.iop.org/0953-8984/9/35/019)

J. Phys.: Condens. Matter **9** (1997) 7463–7468. Printed in the UK PII: S0953-8984(97)78688-0

Structure and magnetic properties of $La_{1-x}Ce_xFe_{10.4}Si_{2.6}$ compounds

Yanming Zhao†, Jingkui Liang†‡, Guanghui Rao†, Weihua Tang†§ and Yongquan Guo†

† Institute of Physics and Centre for Condensed Matter Physics, Chinese Academy of Sciences, PO Box 603, Beijing 100080, People's Republic of China

‡ International Centre for Materials Physics, Chinese Academy of Sciences, Shengyang 110015, People's Republic of China

Received 15 October 1996, in final form 14 January 1997

Abstract. The stability, crystal structure and magnetic properties of $La_{1-x}Ce_xFe_{13-y}Si_y$ have been investigated by x-ray powder diffraction and magnetic measurements. With increasing Ce content x, the solubility y of the Si and the stability of the $NaZn_{13}$-type structure decrease. The crystal structure of $La_{0.4}Ce_{0.6}Fe_{10.4}Si_{2.6}$ was refined by the Rietveld method. The refined result indicates that Si atoms preferentially occupy the 96(i) positions in the $NaZn_{13}$-type structure. The substitution of Ce for La in $LaFe_{10.4}Si_{2.6}$ results in a compression of the lattice cell volume and a decrease of the Curie temperature and the saturation magnetization. Taking the free ion value for the moment of the Ce^{3+} ($\mu_{Ce^{3+}} = 2.1\ \mu_B$), the moment of the Fe atom was derived according to the antiparallel coupling model. The calculated results indicate that the moment of the Fe atom is weakly dependent on the value of x.

1. Introduction

Since the discovery of the excellent permanent magnetic material $Nd_2Fe_{14}B$ [1], a worldwide search for other rare-earth transition metal intermetallic magnets has been carried out. It is believed that there exist other compounds in the still unexploited reservoir of ternary compounds containing rare-earth elements R and transition metals [2]. The emergence of $RFe_{1-x}M_x$ (M = Ti, V, Cr, Mo, W, or Si) compounds with $ThMn_{12}$-type structure [3] and $R_2Fe_{17}N_x$ (or C_x) compounds with Th_2Zn_{17} or Th_2Ni_{17}-type structure [4, 5] as promising candidates for permanent magnetic encourages the exploration of magnetic materials in the R–T–M system.

In rare-earth (R) transition metal (T) intermetallic compounds, the strong magnetic coupling between 3d atoms gives rise to a large magnetization. Thus it seems that the novel R–T intermetallic compounds with excellent magnetic properties are always related to a high content of 3d transition metal. $LaCo_{13}$ is the only stable binary compound with the highest content of transition metal among all binary R–T systems. By substituting Al or Si for part of the transition metal Fe, an iron-based cubic $NaZn_{13}$-type structure can be stabilized [6–8]. Motivated at least in part by the potential economic attractiveness of permanent magnets based on $R(Fe, M)_{13}$ (R = rare earth, M = metal or metalloid), a substantial amount of research continues to focus on the effect of elemental substitution in

§ Corresponding author; e-mail: whtang@aphy02.iphy.ac.cn

0953-8984/97/357463+06$19.50

the $NaZn_{13}$ or $NaZn_{13}$-type derived structure. In our previous report [9], $CeFe_{13-x}Si_x$ was obtained in the region of $2.4 \leqslant x \leqslant 2.6$ in as-cast samples. When the as-cast samples were annealed below 800 °C, $CeFe_{13-x}Si_x$ decomposed into $CeFe_2Si_2$ and α-Fe. $LaFe_{13-x}Si_x$, however, can be formed in a wide region of $1.4 \leqslant x \leqslant 5.0$ [10]. Thus a continuous solid solution between $CeFe_{13-x}Si_x$ and $LaFe_{13-x}Si_x$ might exist in the region of $2.4 \leqslant x \leqslant 2.6$. It would be helpful to study the effects of substitution of Ce for La on the crystal structure stability and magnetic properties of $La_{1-x}Ce_xFe_{13-y}Si_y$.

2. Experimental procedures

A series of $La_{1-x}Ce_xFe_{10.4}Si_{2.6}$ samples was prepared by arc melting the appropriate amounts of the starting materials in an atmosphere of ultrapure argon gas. The purity of the four starting elements is better than 99.9%. Excesses of 5% La and 5% Ce were added to compensate the mass loss due to the evaporation of rare-earth elements during melting. The samples were remelted several times to ensure homogeneity. The resulting samples were annealed in vacuum at 1350 K for 12 h.

The phase identification of the samples was carried out by x-ray powder diffraction, using a four-layer monochromatic focusing Guinier–de Wolff camera with Co Kα radiation. High-purity Si powder was used as an internal standard for measurement of the lattice parameter. The diffraction intensity data for structure analysis were collected by an MXP 18A-HF diffractometer with rotating anode, which had an 18 kW x-ray generator and Cu Kα radiation. A graphite monochromator was used for the diffracted beam. The x-ray diffraction (XRD) pattern of $La_{0.4}Ce_{0.6}Fe_{10.4}Si_{2.6}$ was collected by a step scanning mode with a scanning step of 0.02° and a sampling time of 2 s.

The Curie temperatures T_C of $La_{1-x}Ce_xFe_{10.4}Si_{2.6}$ were derived from low-field ac susceptibility curves which were measured using a sensitive mutual inductance technique operating at a frequency of 320 Hz with a driving field of less than 0.1 mT between 77 and 300 K. The saturation magnetizations of the $La_{1-x}Ce_xFe_{10.4}Si_{2.6}$ compounds were determined by an extracting sample magnetometer.

3. Results and discussion

3.1. Stability and crystal structure

XRD patterns of the as-cast samples revealed that almost single-phase samples with $NaZn_{13}$-type structure were obtained in $La_{1-x}Ce_xFe_{10.4}Si_{2.6}$ with $0 \leqslant x \leqslant 1.0$. After annealing at 800 °C for about 1 month, the samples with $x = 0.0$–0.7 are still of single-phase character. In the region of $x = 0.8$–1.0, the amount of the impurity phases ($(La, Ce)Fe_2Si_2$ and α-Fe) increases with increasing Ce content x. Figure 1 shows two typical XRD patterns of $La_{0.4}Ce_{0.6}Fe_{10.4}Si_{2.6}$ (a) and $La_{0.2}Ce_{0.8}Fe_{10.4}Si_{2.6}$ (b) annealed at 800 °C. Comparing figure 1(b) and (a) we found that the diffraction peaks of the $NaZn_{13}$ phase for the sample with $x = 0.8$ broaden obviously, indicating a distortion of the cubic symmetry caused by a partial decomposition of the sample.

In our previous report [9], $CeFe_{13-y}Si_y$ was obtained in the region of $2.4 \leqslant y \leqslant 2.6$ in as-cast samples. When the as-cast samples were annealed below 800 °C, $CeFe_{13-y}Si_y$ decomposed into $CeFe_2Si_2$ and α-Fe. $LaFe_{13-y}Si_y$, however, can be formed in a wide region of $1.4 \leqslant y \leqslant 5.0$ [10]. For a solid solution phase between $CeFe_{13-y}Si_y$ and $LaFe_{13-y}Si_y$, the stable region of $NaZn_{13}$-type structure at high temperature should be larger than $2.4 \leqslant y \leqslant 2.6$, but smaller than $1.4 \leqslant y \leqslant 5.0$. The possible stable region is

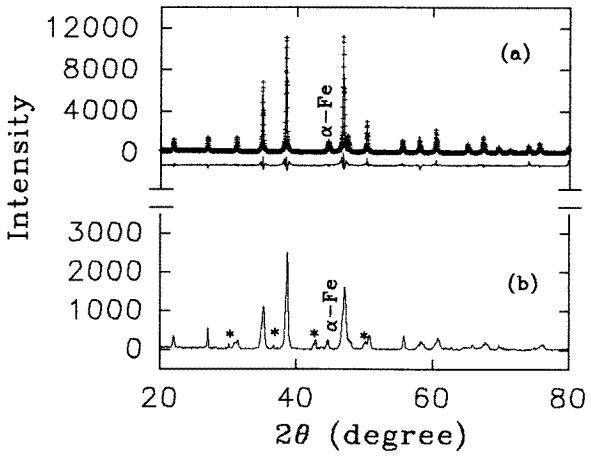

Figure 1. The XRD patterns (Cu Kα radiation). (a) The output from Rietveld analysis of $La_{0.4}Ce_{0.6}Fe_{10.4}Si_{2.6}$. The observed data are indicated by crosses and the calculated profile is the continuous line overlaying them. The lower curve is the difference between the observed and calculated intensities at each step, plotted on the same scale and shifted a little downwards for clarity. (b) The XRD pattern of $La_{0.2}Ce_{0.8}Fe_{10.4}Si_{2.6}$. The asterisks indicate (La, Ce)Fe_2Si_2.

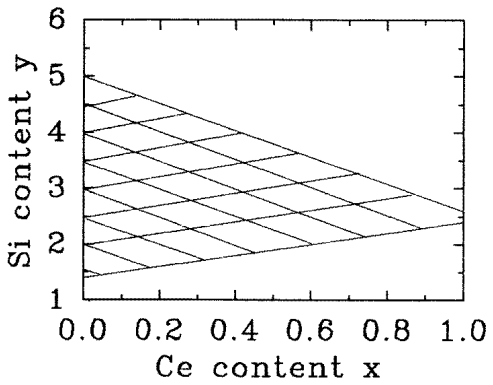

Figure 2. A schematic diagram of the stable region of $La_{1-x}Ce_xFe_{13-y}Si_y$ at high temperature.

shown as the shaded part in figure 2. When $y < 2.4$ and $y > 2.6$, the substitution of Ce for La decreases in $La_{1-x}Ce_xFe_{13-y}Si_y$. After annealing the samples at 800 °C for 1 month, a metallic bright core and a grey shell were formed in the samples with $x = 0.8$–1.0. The XRD patterns show that the core is almost a single phase with $NaZn_{13}$-type structure (figure 1(b)), while the shell mainly consists of (La, Ce)Fe_2Si_2 and α-Fe. This feature might be attributed to an incompleteness of the phase decomposition controlled by the dynamic process. All the following results refer to the core part in the samples.

The lattice constants of $La_{1-x}Ce_xFe_{10.4}Si_{2.6}$ compounds listed in table 1 were determined by indexing the XRD patterns using the TREOR program and refined using the PIRUM program. The composition dependence of the lattice constants is shown in figure 3. With increasing Ce content x, the lattice constant decrease linearly, $a(x) = 11.439 - 0.106x$, and follows the Vegard law very well, indicating that the decomposition of $La_{1-x}Ce_xFe_{10.4}Si_{2.6}$

Table 1. The magnetic and lattice parameters for $La_{1-x}Ce_xFe_{10.4}Si_{2.6}$.

x	$a \pm 0.002$ (Å)	$T_C \pm 2$ (K)	$M_{exp} \pm 0.006$ (μ_B/fu)	$\mu_{Fe} \pm 0.001$ (μ_B/fu)
0	11.439	239	18.632	1.792
0.1	11.425	236		
0.2	11.418	231	18.473	1.816
0.3	11.407	230		
0.4	11.394	226	18.191	1.829
0.5	11.386	224		
0.6	11.380	221	17.824	1.835
0.7	11.364	217		
0.8	11.350	215	17.010	1.797
0.9	11.342	212		
1.0	11.333	209	16.563	1.794

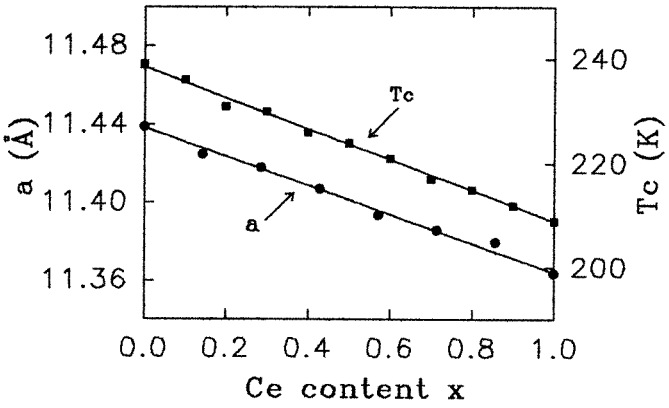

Figure 3. The concentration dependence of the Curie temperature T_C and the lattice constant a of $La_{1-x}Ce_xFe_{10.4}Si_{2.6}$.

($x > 0.8$) into $(La, Ce)Fe_2Si_2$ and α-Fe does not affect the composition of the core part of $La_{1-x}Ce_xFe_{10.4}Si_{2.6}$. The decrease of the lattice constant from $LaFe_{10.4}Si_{2.6}$ to $CeFe_{10.4}Si_{2.6}$ is 0.9%.

Table 2. Refined atomic parameters of $La_{0.4}Ce_{0.6}Fe_{10.4}Si_{2.6}$.

Atom	Position	x	y	z	Occupied number
La	8(a)	0.25	0.25	0.25	3.2(5)
Ce	8(a)	0.25	0.25	0.25	4.8(5)
Fe	8(b)	0.0	0.0	0.0	8
Fe	96(i)	0.0	0.1790(2)	0.1169(2)	75.2(5)
Si	96(i)	0.0	0.1790(2)	0.1169(2)	20.8(5)

The crystal structure of $La_{0.4}Ce_{0.6}Fe_{10.4}Si_{2.6}$ was analysed using the Rietveld method [11]. Since α-Fe was identified as an impurity in the sample, we refined the XRD pattern on the basis of two phases. The space group of the cubic $NaZn_{13}$-type structure is $Fm3c$. The number of chemical formulae per unit cell is eight. The output patterns from Rietveld

Table 3. The bond lengths of $La_{0.4}Ce_{0.6}Fe_{10.4}Si_{2.6}$.

Atom	Atom	Bond length (Å)
R[a]	24X[b]	3.32(3)
Fe	12X	2.43(2)
X	2R	3.32(3)
	1Fe	2.43(2)
	9X	2.53(2)

[a] R = (0.4La + 0.6Ce).
[b] X = (75.2Fe + 20.8Si)/96.

analysis are shown in figure 1(a). The final residual factor R_{wp} is 15.2%. The refined atomic parameters of $La_{0.4}Ce_{0.6}Fe_{10.4}Si_{2.6}$ are listed in table 2. The 8(a) positions are randomly occupied by 3.2La + 4.8Ce, the 8(b) positions by 8Fe, and the 96(i) positions by 75.2Fe + 20.8Si randomly. The bond lengths are listed in table 3.

3.2. Magnetic properties

Ac susceptibility measurements indicate that all samples of $La_{1-x}Ce_xFe_{10.4}Si_{2.6}$ ($x = 0$–1.0) are of a ferromagnetic character. The Curie temperatures T_C are presented in figure 3 and table 1. It is found that the Curie temperature decreases linearly with increasing Ce content x, $T_C(x) = 239 - 30x$. The magnetization curves at 4.2 K for $La_{1-x}Ce_xFe_{10.4}Si_{2.6}$ ($x = 0.0$, 0.2, 0.4, 0.6, 0.8 and 1.0) are shown in figure 4. The saturation magnetizations, which are listed in table 1, are derived from the magnetization curves. With increasing Ce content, the saturation magnetization decreases. Tang *et al* found that nitrogenation of $LaFe_{13-y}Si_y$ resulted in a large lattice expansion and an increase of the Curie temperature and spontaneous magnetization [12]. For $La_{1-x}Ce_xFe_{10.4}Si_{2.6}$, the cell volume is compressed from $x = 0.0$ to $x = 1.0$ by 2.8% and the Curie temperature and the saturation magnetization decreased by 12.6 and 11.1% respectively. Our results are in concordance with the nitrogenation effect of Tang *et al*. Since the Fe content is fixed, the decrease of the saturation magnetization must be caused by the substitution of Ce for La. The substitution of Ce results in a compression of the lattice cell volume, and this compression can also result in the decrease of the saturation magnetization. If we only consider the lattice effect similar to the nitrogenation effect in $LaFe_{10.6}Si_{2.4}$, the cell volume contraction from $LaFe_{10.4}Si_{2.6}$ to $CeFe_{10.4}Si_{2.6}$ would lead to a decrease of 3.1% for the saturation magnetization, which is much lower than the experimental value. Therefore, the moment of Ce^{3+} seems to make some contribution to the saturation magnetization of $La_{1-x}Ce_xFe_{10.4}Si_{2.6}$. Since La does not make any contribution to the magnetization of $LaFe_{10.4}Si_{2.6}$ we can derive the magnetic moment per Fe atom to be 1.792(1) μ_B from the saturation magnetization of $LaFe_{10.4}Si_{2.6}$. The antiparallel coupling between the moment of Fe and that of Ce^{3+} could result in a decrease of the saturation magnetization. Assuming the moment of the Ce^{3+} is equal to the free ion value ($\mu_{Ce^{3+}} = 2.1\ \mu_B$), we can simply derive the moment of the Fe atom by the antiparallel coupling model ($M_{exp} = 10.4\ \mu_{Fe} - x\mu_{Ce^{3+}}$). The calculated results are listed in table 1. The average moment of the Fe atom is 1.180(1) μ_B. The calculated results indicate that the moment of the Fe atom is weakly dependent on the value of x. Since a small amount of impurities resulting from the decomposition process is included in the samples for $x > 0.8$, the saturation magnetization might be a little lower than its real value. Therefore, the saturation magnetization decreases more rapidly for $x > 0.8$.

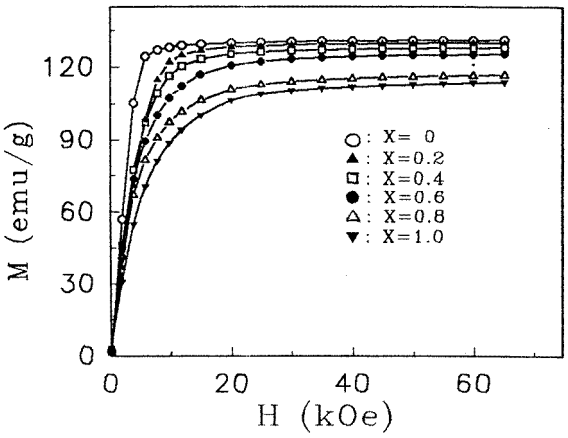

Figure 4. Magnetization curves of $La_{1-x}Ce_xFe_{10.4}Si_{2.6}$.

4. Conclusion

The stability, crystal structure and magnetic properties of $La_{1-x}Ce_xFe_{13-y}Si_y$ have been investigated by x-ray powder diffraction and magnetic measurements. With increasing Ce content x, the solubility y of the Si and the stability of the $NaZn_{13}$-type structure decrease. The crystal structure of $La_{0.4}Ce_{0.6}Fe_{10.4}Si_{2.6}$ was refined by the Rietveld method. The refined result indicates that Si atoms preferentially occupy the 96(i) positions. The substitution of Ce for La in $LaFe_{10.4}Si_{2.6}$ results in a compression of the lattice cell volume and a decrease of the Curie temperature and the saturation magnetization. The effect of the substitution of Ce for La is similar to the effect of nitrogenation in $La(Fe, Si)_{13}$ compounds.

Acknowledgment

This work was supported by the National Natural Science Foundation of China.

References

[1] Sagawa M, Fujimura S, Togawa M and Matsuura Y 1984 *J. Appl. Phys.* **55** 2083
[2] Buschow K H J 1991 *Rep. Prog. Phys.* **54** 1123
[3] Li Schou-Hong and Coey J D M 1991 *Ferromagnetic Materials* vol 6, ed K H J Buschow and E P Wohlfarth (Amsterdam: North-Holland) p 1
[4] de Mooij D B and Buschow K H J 1988 *J. Less-Common Met.* **142** 349
[5] Hong Sun, Coey J M D, Otani Y and Hurley D P F 1990 *J. Phys.: Condens. Matter* **2** 6465
[6] Kripyakevich P I, Zarechnyuk O S, Hladyschevsky E I and Bodak O I 1968 *Z. Anorg. Chem.* **90**
[7] Palstra T T M, Nieuwenhuys G J, Maudosh J A and Buschow K H J 1985 *Phys. Rev.* B **31** 4622
[8] Palstra T T M, Mydosh J A, Nieuwenhuys G J, van der Kraan A M and Buschow K H J 1983 *J. Magn. Magn. Mater.* **36** 290
[9] Zhao Y M, Liang J K, Tang W H, Guo Y Q and Rao G H 1995 *J. Appl. Phys.* **78** 2866
[10] Tang W H, Liang J K, Rao G H and Yan X H 1994 *Phys. Status Solidi* **141** 217
[11] Wiles D B, Sakthivel A and Yang R A 1990 *User's Guide to Program DBW3.25-PC9005 for Rietveld Analysis of X-ray and Neutron Powder Diffraction Data*
[12] Tang X Z, Deng X H, Hadjipanayis G C, Paraefthymiou V and Sellmyer D J 1969 *IEEE Trans. Magn.* **MAG-29** 2839